Original article

Findings in children severely infected with a novel influenza A virus of swine origin: pulmonary imaging

Wei Xu, Chun-Feng Liu, Ying Zhao, Jiu-Jun Li, Li-Jie Wang, Guang-Fu Wen, Zhe Liu
Shenyang, China

Background: **This article reviews the chest radiography of children with severe infection caused by a novel influenza A (H1N1) virus of swine origin (S-OIV). We analyzed the role of their pulmonary images in predicting the severity and diagnosis of the disease.**

Methods: **Among 97 patients with confirmed novel H1N1 infection, 42 patients treated with mechanical ventilation formed group 1, and the remaining 55 patients constituted group 2. The initial and subsequent radiograhic findings in groups 1 and 2 were compared with respect to the pattern, distribution, and extent of the abnormality.**

Results: **In group 1, 24 patients presented with three or more lung zone diseases, whereas only 5 patients in group 2 demonstrated these findings ($P<0.001$). A pneumomediastinum or pneumothorax was observed in 24/42 patients in group 1 and in 18/55 patients in group 2 ($P=0.019$). Twelve patients in group 1 and 5 in group 2 developed a ground-glass opacity cyst with a honeycomb appearance ($P=0.007$).**

Conclusions: **The most common radiographic and computed tomography findings in children who were severely infected with S-OIV included unilateral or bilateral ground-glass opacities with or without associated focal or multifocal areas of consolidation. Children with bilateral involvement or with greater opacity on the chest radiographs were more likely to worsen and require the mechanical ventilation.**

World J Pediatr 2012;8(3):240-246

Key words: **chest radiography;**
children;
H1N1;
infectious diseases;
pneumonia

Introduction

In late March 2009, the outbreak of a respiratory illness in Mexico was later proved to be caused by a novel influenza A (H1N1) virus of swine origin (S-OIV).[1] At the start of winter in southern hemisphere, the virus was spread to China and resulted in approximately 80% influenza cases.[2] Most patients infected by influenza A virus of S-OIV typically presented with fever, cough, sore throat, chills, headache, rhinorrhea, shortness of breath, myalgia, arthralgia, fatigue, vomiting, or diarrhea; however, some patients demonstrated severe course of infection that might result in respiratory failure and death.[3,4] The spread of the virus to China also affected a large number of pediatric patients, many of whom were admitted to pediatric intensive care units (PICU). A proportion of these patients presented, or developed, severe acute respiratory distress syndrome (ARDS). Therefore, it is essential for clinicians to recognize the possible cases of pandemic H1N1 influenza in high-risk groups, thereby allowing the selection of the appropriate diagnostic tests, specific antiviral therapy, and intensive supportive measures as necessary. The role of radiographic images in epidemic detection and response is evolving with the use of imaging as a tool to identify, predict or diagnose severe cases.[5,6]

Descriptions of the radiological manifestations of S-OIV have been limited to a few case reports.[3,7,8] In this article, we review the chest radiographic and CT findings in pediatric patients with confirmed S-OIV H1N1 infection who were treated at a PICU in China.

Methods

Study population

This study was approved by our institutional review

Author Affiliations: Department of Pediatrics, Shengjing Hospital of China Medical University, No. 36 Sanhao Street, Heping District, Shenyang 110004, Liaoning, China (Xu W, Liu CF, Zhao Y, Li JJ, Wang LJ, Wen GF, Liu Z)

Corresponding Author: Chun-Feng Liu, MD, Department of Pediatrics, Shengjing Hospital of China Medical University, No. 36 Sanhao Street, Heping District, Shenyang 110004, Liaoning, China (Tel: +8602423692117; Fax: +8602483955509; Email: xuw@sj-hospital.org)

doi: 10.1007/s12519-012-0364-2

board with a waiver of informed consent. The study population included all patients with influenza-like illnesses, pneumonia and a positive test result using reverse transcriptase polymerase chain reaction (RT-PCR) for H1N1 virus who were presented to the PICU of Shengjing Hospital Affiliated with China Medical University between September 2009 and January 2010. Ninety-seven children who underwent chest radiographic imaging and/or CT constituted the study population. The study population consisted of 59 boys and 38 girls with a mean age of 3.9 years (range: 8 months to 13 years). The patients were divided into two groups. Group 1 comprised 42 patients who developed a rapid, severe respiratory failure that was unresponsive to helmet-CPAP and required intubation and mechanical ventilation (MV). Group 2 comprised the remaining 55 patients who manifested dyspnea and required hospitalization but no invasive MV. Given the different clinical course between the two groups, the radiographic findings in each group were described separately.

Radiographic assessment

Most of the images were reviewed on a PACS viewer with a 2560 × 2048 pixel monitor workstation. Some of the chest radiographic images were taken in a local hospital or in a clinic at our hospital, and were unable to be reviewed by PACS, then we performed additional imaging. When the illness was too severe for patients to be moved out of PICU, portable radiographic examinations were performed with digital radiography equipments using a standardized technique. Ninety-seven patients had follow-up chest radiography (42 in group 1 and 55 in group 2) within one week of the initial chest radiographic imaging. In patients whose illness progressed quickly but the condition remained well or the death risk was low, CT scan was performed. If the condition of the patient was instable, CT scans should not be performed. Chest CT examinations were performed in 63 patients (18 in group 1 and 45 in group 2; children in group 1 were too serious to be taken out for CT scans, so CT scans in group 1 were less than in group 2). Radiographs and CT scans were assessed by trained radiologists of radiology department who were not involved in the analysis for the presence of ground-glass opacities, consolidation, a tree-in-bud pattern, reticular opacities and honeycomb lung. The presence of associated hilar, mediastinal, or pleural abnormalities was also assessed. Ground-glass opacities were defined as hazy areas of increased opacity or attenuation without obscuring of the underlying vessels. Consolidation was defined as a homogeneous opacity of the parenchyma with obscuring of the underlying vessels. Reticular opacities were defined as linear opacities that formed a mesh-like pattern. Honeycomb lung was defined as the radiological and gross appearance of the lungs resulting from diffuse fibrosis and cystic dilation of bronchioles. The involvement was categorized as unilateral or bilateral. If the involvement was deemed bilateral, the process was categorized as symmetric or asymmetric in nature. Each lung was divided into upper, middle, and lower lung zones (each comprising a third of the craniocaudal extent of the lungs on a frontal radiograph), and the zonal involvement was assessed. The extent of abnormality was subjectively graded as the percentage of each lung involved, and an average was calculated for each radiographic study. The distribution was categorized as 1/4 quadrants per lung in total, 2/4 quadrants and 3/4 or more involved zones of one lung. A predominant distribution was also assessed with respect to location in the upper, middle, or lower lung zone. Both groups demonstrated a high ratio of pneumomediastinum or pneumothorax. Based on the site, we classified the radiographic findings into mediastinal emphysema, cutaneous emphysema and pneumatothorax.

Statistical analysis

Data analysis was conducted using SPSS 13.0 software. Discrete variables were expressed as counts (percentages) and continuous variables as means ± standard deviation (SD) or medians in the 25th to 75th interquartile range (IQR). For the demographic and clinical characteristics of the patients, differences between the groups were assessed using the chi-square test for categorical variables and Student's *t* test or the Mann-Whitney *U* test for continuous variables. A *P* value ≤0.05 was considered statistically significant.

Results

General characteristics of the study population

The patients in group 1 were younger (mean: 3.43 years *vs*. 4.5 years, independent samples *t* test) than those in group 2. The male to female ratio was 8:6 in group 1 and 7:4 in group 2 (P=0.742, the chi-square test). Five deaths occurred in group 1 (5/42). Two patients were complicated with diffuse alveolar hemorrhage and severe pneumatothorax; one of them succumbed to respiratory failure 8 hours after admission (Fig. 1), and the other died after 24 days on MV. The third death happened 5 days after admission in a 12-year-old girl who had had systemic lupus erythematosus. The remaining 2 patients died from severe sepsis due to a secondary infection. All the patients in group 2 recovered completely.

Analysis of chest radiography

We examined the chest images of the children who underwent serial imaging consecutively after hospitalization in the PICU. The initial chest radiographic images available for review were obtained at an average of 5.1 days (range: 2-9 days) after the onset of clinical symptoms, at clinic visit or on hospital admission. The mean time from initial symptoms to the first obtained imaging study in group 1 was 5.0 days, whereas it was 5.3 days in group 2 (P>0.05). The mean time from admission to the onset of MV was 18 hours (0-70 hours), and to the chest radiographic examination was 2 days (1-5 days) for mechanically ventilated group 1. The imaging findings are summarized in the Table.

Among the 42 patients who received MV, the median length of hospital stay was 19 days (range: 1-56) as compared with 14 days (range: 6-20) in group 2 (P=0.073).When the patients were admitted to the PICU, chest radiographic examination was performed. The calculated mean times for obtaining the chest radiograph after admission was 6.71 in group 1 and 3.36 in group 2 (P<0.001). The lung abnormalities were bilateral in 33 (78.6%) patients in group 1, and in 50 (90.1%) patients in group 2. Initial chest radiography revealed no significant differences between the two groups. However, 9 patients in group 1 showed a bilateral abnormality on the radiographic images within a week (Fig. 2). The pattern of radiographic abnormality was evaluated when the patients were in the most serious conditions, i.e., the degree of hypoxemia was worst or vent settings were most high. Based on abnormalities in chest radiography, the ratio of local patchy shadowing (Fig. 2A, 3A, 3B) to ground-glass opacities (Fig. 2D, 3D) was found to be 47:50. The percentage of ground-glass opacities was 71.4% in group 1 and 36.4% in group 2 (P<0.001). Lung abnormalities were most commonly detected in the lower and central lung zones (41/97 and 43/97 respectively), but there was no difference in the two

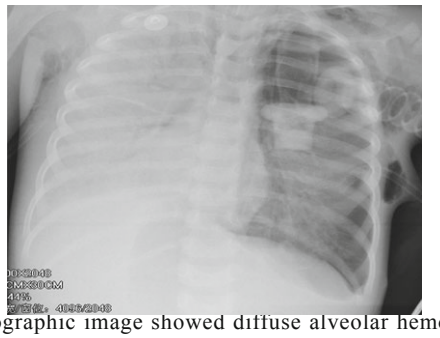

Fig. 1. Radiographic image showed diffuse alveolar hemorrhage (obviously in the right lung) and a severe pneumatothorax (left lung) in a patient who died from respiratory failure 8 hours after admission.

Table. Summary of radiographic and CT findings in H1N1 S-OIV-infected children

Patients with confirmed H1N1 S-OIV		Group 1 (n=42)	Group 2 (n=55)	All (n=97)	P value
Days from symptom onset to first radiographic image	Mean	5.0±2.04	5.3±2.12	5.1±2.07	>0.99
	Range	2-9	2-8	2-9	
Length of hospital stay (d)	Median	19	14	17	0.073
	Range	1-56	6-20	1-56	
Times of chest radiography after admission* (vic)	Mean	6.71	3.36	5.44	0.032
	Range	1-18	1-4	1-18	
Distribution (the first radiographic images)	Unilateral involvement on chest radiograph†	9 (21.4%)	5 (9.1%)	14 (14.4%)	0.206
	Bilateral involvement on chest radiograph	33 (78.6%)	50 (90.1%)	83 (85.6%)	
Pattern of radiographic abnormality (the clinical situation was most severe)	Local patchy shadowing	21 (50.0%)	35 (63.6%)	56 (57.7%)	0.000
	Ground-glass opacities	21 (50.0%)	20 (36.4%)	41 (42.3%)	
Predominance‡	Upper zone	3 (7.1%)	10 (18.2%)	13 (13.4%)	0.639
	Central zone	18 (42.9%)	25 (45.5%)	43 (44.3%)	
	Lower zone	21 (50.0%)	20 (36.4%)	41 (42.3%)	
Opacity in initial chest X-ray	1/4 quadrants	6 (14.3%)	35 (63.6%)	41 (42.3%)	0.0172
	2/4 quadrants	12 (28.6%)	15 (27.3%)	27 (27.8%)	
	3/4 quadrants or more involved zones	24 (57.1%)	5 (9.1%)	29 (29.9%)	
Pneumatothorax and pneumohypoderma	Pneumatothorax	9 (21.4%)§	3 (5.5%)	12 (12.4%)	0.111
	Pneumohypoderma	15 (35.7%)‖	15 (27.3)	30 (30.9%)	
Ground-glass opacity cyst on CT		12 (28.6%)	5 (9.1%)	17 (17.5%)	0.148

*: Children with acute respiratory distress syndrome would be managed by obtaining a radiograph every day or every other day during the early stages of disease; children with frequent hemorrhoid would be managed by obtaining a radiograph at any time according to the condition of the patient. †: Two children showed an unilateral distribution within one week of symptom. ‡: The pathologic process in some images was not discriminated easily as center or lower lung zones, thus one zone was selected according to the sick area in each zone. §: Three of the nine patients developed pneumatothorax prior to mechanical ventilation, including one child who died after 8 hours of hospitalization. ‖: Three of the 15 patients developed pneumohypoderma prior to mechanical ventilation.

groups. There were diffuse abnormalities on chest radiographies of the 9 patients in group 1 and 6 patients in group 2. CT therefore could distinguish the lung zone that was predominantly affected (Figs. 2-4). The extent of the disease was greater in the group 1 patients that required MV, demonstrating the involvement of three or more lung zones in 24/42 (57.1%) patients as compared with 5/55 (9.1%) of the patients in group 2. In addition, the overall extent of lung involvement was 2/4 in 12 patients in group 1 in contrast to 15 patients in group 2. The extent of lung involvement was 1/4 quadrants in 6 patients of group 1 versus 35 patients of group 2 (P<0.001). Pneumatothorax and pneumohypoderma were the most common complications (Fig. 4). Mediastinal emphysema was usually followed by pneumohypoderma. Irrespective of whether the patients had undergone MV, they should present pneumomediastinum or pneumothorax, therefore, there was no relationship between MV and pneumomediastinum or pneumothorax. This condition was observed in 24 and 18 patients in groups 1 and 2, respectively (P=0.019). Pulmonary interstitial emphysema occurred almost exclusively in association with MV. Extensive cystic and linear densities were noted and were thought to represent pulmonary interstitial emphysema and fibrosis respectively. After prolonged treatment, the patients survived, but multiple cysts formed in their lungs. Neither chest radiograph nor chest CT showed pleural effusions.

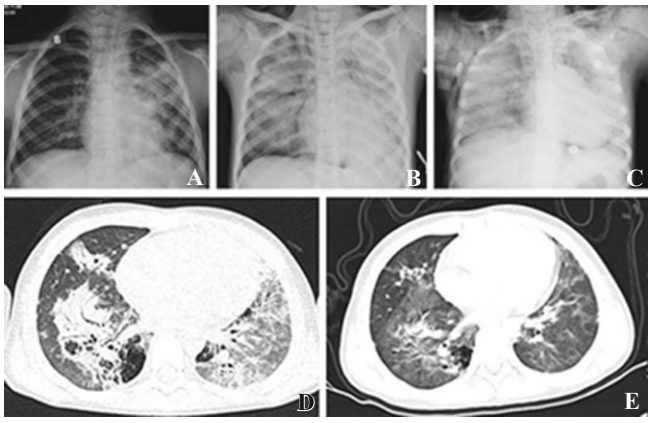

Fig. 2. Radiographic and CT findings in a 10-year-old girl. **A:** Four days after onset of symptoms (the first admission day), the first radiograph showed patchy air-space consolidation in the left middle lung zone associated with ill-defined nodules. Mild consolidation is evident in the right lower lobe. **B:** Three days after admission, the lesion of the lungs spread rapidly. The radiograph showed diffuse bilateral alveolar infiltrates, indistinct margins, tendency to coalesce, and the presence of air bronchogram or silhouette sign (effacement of an anatomical soft-tissue border due to adjacent consolidation). Spontaneous mediastinal emphesema was seen on the chest radiograph. **C:** Ten days after admission, after 7 days of MV, secondary infection of *Pseudomonas aeruginosa* in the lung was found. The chest radiograph showed diffuse alveolar infiltrates. **D:** CT scan showed air bronchogram, ground-glass opacity, bilateral air-space consolidation and multi cysts after 20 days of hospital stay. **E:** Two months after discharging from hospital, CT scan showed that multi cysts were present with diffuse lung grand-glass opacities, compared with **D**.

CT in patients with severe lung disease

The patients with CT abnormalities presented with abnormal findings on chest radiographs. CT scans were performed in 63 patients (64.9%) and showed airspace consolidation and a ground-glass opacity that demonstrated a multilobar and bilateral distribution. However, the extent of involvement was more diffuse, and the distribution of the disease was better characterized on CT. Before a child was cured, chest CT would display some insidious processes such as cysts and fibrosis, which exhibited a honeycombing appearance or signified that some patients would develop bronchiolitis obliterans. In these patients, 17 (12 in group 1 and 5 in group 2) demonstrated honeycombing appearance on their lungs after long-term treatment (18-46 days after admission) (Figs. 2, 3).

Discussion

Influenza viruses have a multipartite, negative-sense, and single-stranded RNA genome and a lipid envelope. They are divided into 3 genera, A, B and C, within the family *Orthomyxoviridae*, based on the antigenic properties of the viral nucleoprotein. Influenza B and C viruses principally infect humans. They typically cause mild illness in children and undergo only gradual antigenic variation.[9] By contrast, the influenza A viruses are capable of infecting the human respiratory tract, and the periodic emergence of antigenically novel agents through genomic reassortment enables influenza A viruses to cause periodic worldwide epidemics with high morbidity and mortality ("pandemic influenza").

In June 2009, the World Health Organization raised the pandemic alert level to phase 6 because of the spread of the disease to all continents.[10] The effect that the swine-originating influenza H1N1 virus will have on global child health is currently unknown. There have been attempts to predict outcomes by extrapolating from knowledge of related viruses and adult data.[3,11,12] Most of the published clinical reports regarding the features of patient chest radiographic images could provide useful information about these patients, but information on the pediatric specialty is rare. In this study, we analyzed the radiographic images of 97 severe pediatric patients.

The medical literature contains few presentations of radiographic findings in seasonal influenza, possibly because of the non-specificity of this condition and the frequent confounding features due to co-infection

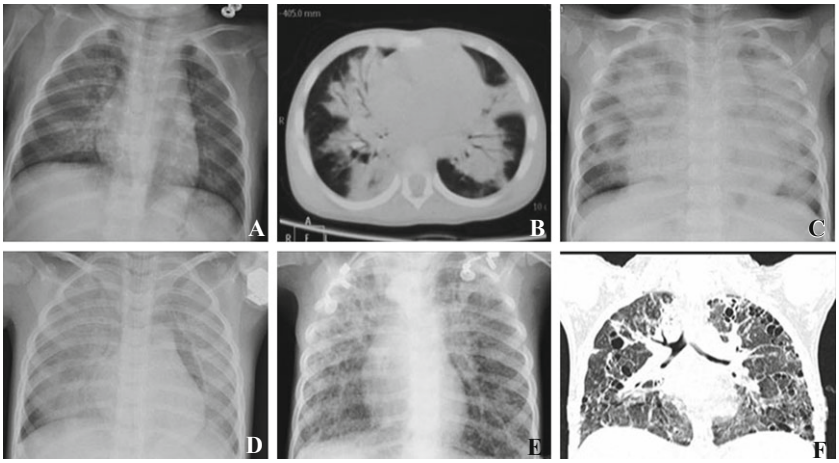

Fig. 3. Radiographic and CT findings in a 3-year-old boy. **A:** The first chest radiograph taken at 5 days after onset of symptoms showed patchy shadowing in the right lower lung zone. Mild consolidation was evident in the left lung. **B:** Seven days after onset of symptoms (2 days after admission), chest CT showed hilar and vascular radiographic sharpness was lost due to bronchial wall thickening with peribronchial interstitial edema and inflammatory infiltrate. Due to the central airway involvement there were peripheral air trapping and hyperinflation. Patchy pulmonary densities can be seen and are usually due to subsegmental atelectasis. **C:** Eight days after onset of symptoms, ground-glass opacities were observed in the left lung and multiple patchy shadowing in the right lung. **D:** Fourteen days after onset of symptoms, the child developed pneumomediastinum and secondary infection with baumanii. Both lungs showed ground-glass opacities. **E:** The child was on a ventilator for 44 days, follow-up radiography at 50 days after onset of symptoms showed patchy bilateral linear opacities and development of multiple thin-walled cystic lucencies. **F:** CT taken at 59 days after onset of symptoms showed a diffuse pattern of well-circumscribed cysts. The cysts had a diffuse homogeneous appearance throughout the lungs. The lung area between the cysts had a ground-glass opacity on CT. The lung was characterized by irregular linear opacities and honeycombing that involved mainly the subpleural regions.

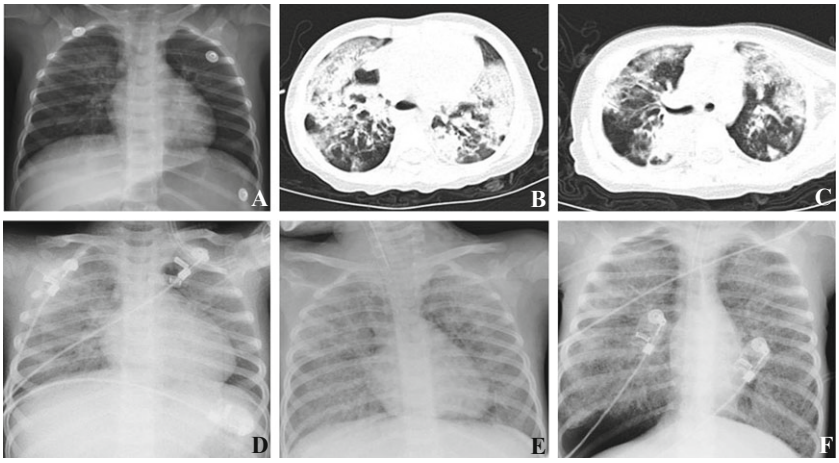

Fig. 4. Radiographic and CT findings in a 4-year-old boy with headache and convulsion who was admitted to the PICU. **A:** The first film taken at 4 days after onset of symptoms showed acute interstitial lung infiltrates with interstitial pulmonary edema and lung marking coarse. **B&C:** Eight days after onset of symptoms, his dyspnea was more severe. CT showed multiple pulmonary nodules of different sizes and with variations in sharpness of nodular margins. Normal lung was limited. **D:** Fourteen days after onset of symptoms, the image showed diffuse ground-glass opacity on both lungs. **E:** Sixteen days after onset of symptoms, after mechanical ventilation for 7 days, bilateral airspace densities and small right pneumothorax and pneumomediastinum were seen. **F:** Forty-four days after onset of symptoms, with deterioration in the child status, pneumothorax on both sides was seen along with three drainage tubes (two in the right lobe and one in the left). Pneumomediastinum and pneumohypoderma were severe. The heart was greatly oppressed by the distended lungs. The patient had a bronchopleural fistula. Mechanical ventilation was given for 55 days and the patient died at 64 days after onset of symptoms.

and multifactorial lung injury; most cases are not sufficiently severe to warrant imaging. Historically, seasonal influenza has been associated with heightened mortality due to superinfection with community acquired pneumonia, in which the radiographic pattern may be lobar and nonsegmental.[13-16] This finding is in contrast to the multifocal patchy peripheral distribution and ground-glass opacities observed herein, corroborating previous preliminary reports in adults.[3,8,17,18] Although some patients presented with a clinically poor situation, their chest radiographic images were only slightly abnormal, and the images changed very quickly as the disease

developed. The abnormalities changed from unilateral to bilateral, single focal areas of consolidation to multifocal, local patchy shadowing and then to diffuse pathological changes. There were more bilaterally abnormalities than unilaterally abnormalities, which might be due in part to the severity of the illness, the decreased immunocompetence of the patients or unconventional treatments before admission. Additionally, comorbidities have complicated the imaging findings.[19-21] Fourteen children in group 1 and 6 children in group 2 demonstrated one or two episodes of hospital-acquired bacterial infections (5 cases of baumani, 5 cases of *Pseudomonas aeruginosa*, 3 cases of *Escherichia coli*, 3 cases of *Pseudomonas maltophilia*, 2 cases of *Staphylococcus aureus* and 2 cases of *Klebsiella pneumoniae*). All of the infections were diagnosed via bronchoalveolar lavage, and the patients were subjected to prolonged treatment, which modified the features of chest radiographic images. In a recently published series of 18 cases of fatal S-OIV infection in Mexico,[3] the investigators reported that patchy bilateral opacities were observed on the radiographs of all patients and that one CT image revealed a ground-glass air-space density. Although that report provided a limited description of the radiographic features of these cases, the findings were consistent with the present results and provided details concerning the characterization of lung injury resulting from S-OIV H1N1.

The pneumomediastinum or pneumothorax morbidity in our cases was higher than that reported in previous adult cases.[3,3,8,17,18] Among the patients, 43.1% had pneumatothorax or pneumohypoderma, which was spontaneous in 23 children. Another 19 children presented with an accompanying pneumomediastinum or pneumothorax after MV, but we could not confirm the outcome of MV. The viral infection might have led to necrosis of the terminal bronchiole, thus inducing a spontaneous pneumomediastinum or pneumothorax. CT revealed the development of ground-glass opacity cyst in 17 patients after long-term treatment; however, the causes of such result were unclear. A greater number of patients in group 1 developed honeycombing, which may be associated with the severity of the disease and MV. These cases of severe S-OIV infection suggested a noncardiogenic lung injury or ARDS. In ARDS, respiratory epithelial injury with an abnormally increased permeability of the capillary endothelium initially produces patchy consolidations on CTs and radiographs and then evolves into a confluent bilateral air-space opacity. In our patients, ARDS was associated with a pattern of severe lung injury involving alveolitis, interstitial substance damage and peribronchial inflammation. If a child was subjected to chest radiography that showed bilateral lung involvement or a large area of opacity, the probability of MV for the child would be very high. The patients in group 1 were given MV 18 hours after admission, with findings consistent with those of Perez-Padilla, showing that the time from hospitalization to MV might be as short as 24 hours or less.[3] Two patients were complicated with lung hemorrhage in the early phase of the disease and finally died. The incidence of hemorrhage might be related to injury of the alveola caused by virus or macrophages and neutrophils infiltration.[22] Another reason might be the increasing lung artery permeability which was induced by systemic inflammatory response syndrome. Also it might be related with lung artery injury that was caused by virus infection. Besides, high positive end-expiratory pressure in MV could stop the bleeding, which might have something to do with the former reason.

Our study had several limitations. First, it was a retrospective study. Therefore, some materials were not managed in our hospital. Second, not all of the pediatric patients presented a CT correlation. Finally, none of the patients underwent a lung biopsy or an autopsy that would have allowed the determination of a radiographic-histopathologic correlation.

In conclusion, the most common radiographic and CT findings in children who were severely infected with S-OIV were unilateral or bilateral ground-glass opacities with or without associated focal or multifocal areas of consolidation. Children with bilateral involvement or a greater opacity on the chest radiographs were more likely to worsen and require ventilation. MV increased the incidence of pneumomediastinum or pneumothorax. Based on the radiographic data, we were able to immediately discover the extent of pneumomediastinum or pneumothorax. The ground-glass opacities and areas of consolidation exhibited a predominantly peribronchovascular and subpleural distribution on the CT that resembled the appearance of developing pneumonia. Laterally, the chest CT displayed some insidious processes such as ground-glass opacity cyst (honeycombing), which signified that some patients would develop bronchiolitis obliterans, and these features were not easily identified on the chest radiograph.

Funding: None.
Ethical approval: This study was approved by the data inspectorate of China and by the regional committee for medical research ethics.
Competing interest: None declared.
Contributors: Xu W collected, analyzed and interpreted the data, provided statistical analysis and wrote the manuscript under the supervision of Liu CF. Wen GF and Liu Z collected the data. Wang

LJ and Li JJ discussed and reviewed the manuscript. All authors read and approved the final manuscript. Liu CF is the guarantor.

References

1 World Health Organization, 2009. http://www.who.int/csr/don/2009_04_26/en/index.html (accessed December 20, 2009).
2 Cao B, Li XW, Mao Y, Wang J, Lu HZ, Chen YS, et al. Clinical features of the initial cases of 2009 pandemic influenza A (H1N1) virus infection in China. N Engl J Med 2009;361:2507-2517.
3 Perez-Padilla R, de la Rosa-Zamboni D, Ponce de Leon S, Hernandez M, Quiñones-Falconi F, Bautista E, et al. Pneumonia and respiratory failure from swine-origin influenza A (H1N1) in Mexico. N Engl J Med 2009;361:680-689.
4 U.S. Centers for Disease Control and Prevention Website, 2009. http://www.aatchb.org/nptpp/CDC%20-%20Swine%20Influenza%20Guidance%20for%20Clinicians.pdf (accessed December 20, 2009).
5 Mollura DJ, Carrino JA, Matuszak DL, Mnatsakanyan ZR, Eng J, Cutchis P, et al. Bridging radiology and public health: the emerging field of radiologic public health informatics. J Am Coll Radiol 2008;5:174-181.
6 Gunderman RB, Brown BP. Pandemic influenza. Radiology 2007;243:629-632.
7 Centers for Disease Control and Prevention (CDC). Hospitalized patients with novel influenza A (H1N1) virus infection - California, April-May, 2009. MMWR Morb Mortal Wkly Rep 2009;58:536-541.
8 DiagnosticImaging.com Website. Abella HA. Xrays and CT offer predictive power for swine flu diagnosis. http://www.diagnosticimaging.com/digital-x-ray/content/article/113619/1425699 (accessed December 20, 2009).
9 Doherty PC, Turner SJ, Webby RG, Thomas PG. Influenza and the challenge for immunology. Nat Immunol 2006;7:449-455.
10 WHO headquarters. Influenza A (H1N1): WHO announces pandemic alert phase 6, of moderate severity. http://as.pi.ac.ae/PI_INS/hse/tips/Health/WHO%20updates.pdf (accessed December 20, 2009).
11 Agarwal PP, Cinti S, Kazerooni EA. Chest radiographic and CT findings in novel swine-origin influenza A (H1N1) virus (S-OIV) infection. AJR Am J Roentgenol 2009;193:1488-1493.
12 Centers for Disease Control and Prevention (CDC). Intensive-care patients with severe novel infl uenza A (H1N1) virus infection - Michigan, June 2009. MMWR Morb Mortal Wkly Rep 2009;58:749-752.
13 Sullivan CJ, Jordan MC. Diagnosis of viral pneumonia. Semin Respir Infect 1988;3:148-161.
14 Layne SP, Monto AS, Taubenberger JK. Pandemic influenza: an inconvenient mutation. Science 2009;323:1560-1561.
15 Morens DM, Taubenberger JK, Fauci AS. Predominant role of bacterial pneumonia as a cause of death in pandemic influenza: implications for pandemic influenza preparedness. J Infect Dis 2008;198:962-970.
16 Greenberg SB. Viral pneumonia. Infect Dis Clin North Am 1991;5:603-621.
17 Ajlan AM, Quiney B, Nicolaou S, Müller NL. Swine-origin influenza A (H1N1) viral infection: radiographic and CT findings. AJR Am J Roentgenol 2009;193:1494-1499.
18 Scientific blogging, 2009. http://esciencenews.com/sources/scientific.blogging/2009/05/19/case.reports.of.hospitalized.patients.with.influenza.a.h1n1.swine.flu.in.california.durin (accessed December 20, 2009).
19 Mullooly JP, Barker WH, Nolan TF Jr. Risk of acute respiratory disease among pregnant women during influenza A epidemics. Public Health Rep 1986;101:205-211.
20 Galloway RW, Miller RS. Lung changes in the recent influenza epidemic. Br J Radiol 1959;32:28-32.
21 Tillett HE, Smith JW, Clifford RE. Excess morbidity and mortality associated with influenza in England and Wales. Lancet 1980;1:793-795.
22 Narasaraju T, Yang E, Samy RP, Ng HH, Poh WP, Liew AA, et al. Excessive neutrophils and neutrophil extracellular traps contribute to acute lung injury of influenza pneumonitis. Am J Pathol 2011;179:199-210.

Received July 18, 2011
Accepted after revision December 22, 2011